Effect of Chain Length on the Formation and Stability of Synthetic α-Helical Coiled Coils†

Jeffrey Y. Su, Robert S. Hodges, and Cyril M. Kay*

Department of Biochemistry and the Protein Engineering Network of Centres of Excellence, University of Alberta, Edmonton, Alberta T6G 2H7, Canada

Received September 21, 1994; Revised Manuscript Received October 12, 1994®

ABSTRACT: A series of polypeptides containing 9, 12, 16, 19, 23, 26, 30, 33, and 35 amino acid residues was designed to investigate the effects of peptide chain length on the formation and stability of two-stranded α-helical dimers or coiled coils. These peptides were synthesized by the solid-phase method, purified by reversed-phase high-performance liquid chromatography (RP-HPLC), and characterized by RP-HPLC, amino acid composition analysis, and mass spectrometry. The amphipathic α-helical peptides were designed to dimerize by interchain hydrophobic interactions at positions a and d and interchain salt bridges between lysine and glutamic acid residues at positions e and g of the repeating heptad sequence of Glu-Ile-Glu-Ala-Leu-Lys-Ala (g-a-b-c-d-e-f). The ability of these peptides to form α-helical structures in the presence and absence of a helix-inducing reagent (trifluoroethanol) was monitored by circular dichroism spectroscopy. The helicity of the peptides increased with increasing chain length in a cooperative manner. A minimum of three heptads corresponding to six helical turns was required for a peptide to adopt the two-stranded α-helical coiled coil conformation in aqueous medium. The increased stability of the peptides as a result of an increase in hydrophobic interactions (chain length) was demonstrated by the shift in the transitions of the guanidine hydrochloride (Gdn·HCl) denaturation and thermal unfolding profiles. The concentrations of denaturant (Gdn·HCl) required to achieve 50% denaturation are 3.2, 4.9, 6.9, and 7.5 M for peptides 23r, 26r, 30r, and 33r, respectively, in aqueous medium. However, the effect of a chain length increase on coiled-coil stability was not additive. The melting temperature, T_m, at which 50% of the helicity is lost, increased by 34 °C in changing the peptide chain length from 23 to 26; however, that shift was only 14 °C when the chain length was increased from 30 to 33 residues. These results are consistent with a chain length dependent cooperative folding of the peptides into coiled coils.

One of the outstanding questions in molecular biology and protein engineering, for which we have no clear answer, is how the primary amino acid sequence of a protein determines its three-dimensional structure and its folding pathway. One approach to this problem involves the *de novo* design of model proteins with the desired secondary, tertiary, and quaternary structures. Coiled coils are widely used protein models in this undertaking. The coiled-coil motif, which is formed by the dimerization of two α-helices, is widely observed in biological molecules embracing different shapes and functions in various subcellular or anatomic locations. More than 200 proteins, including fibrous proteins, muscle proteins, DNA-binding proteins, and many disease- and organ-specific autoantigens such as polymyositis and scleroderma antigens, are reported to contain coiled-coiled structures, and many more are expected to be discovered [for reviews, see Talbot and Hodges (1982), Cohen and Parry (1986), Lupas *et al.* (1991), Hodges (1992), Adamson *et al.* (1993), and Dohlman *et al.* (1993)]. As originally proposed by Crick (1953) some 40 years ago, the recent X-ray structure analysis showed that a two-stranded, α-helical coiled coil contains two α-helices that are in a parallel and an in-register alignment and that wrap around each other in a left-handed supercoil (O'Shea *et al.*, 1991).

The simplicity and versatility of the two-helix structure have also made it an attractive target for protein design and protein folding studies (Talbot & Hodges, 1982; Hodges *et al.*, 1981; Lau *et al.*, 1994; Enser *et al.*, 1990; Engel *et al.*, 1991; Zhou *et al.*, 1992a; Moser, 1992). First, it contains only one type of secondary structure, which can be easily studied using spectroscopic methods. Second, it contains two chains, which makes it an ideal model to investigate intermolecular interactions. In addition, although the α-helix has been shown to be the most common fold in proteins, isolated α-helices generally are unstable in water (Wright *et al.*, 1988). Coiled coils therefore have been used as models to examine the α-helix-forming tendencies of amino acids (O'Neil & DeGrado, 1990) and electron transport between helix surface residues (Lee *et al.*, 1992).

Smillie and co-workers first determined the amino acid sequence of a two-stranded, α-helical coiled coil (tropomyosin) and identified the 3,4 (or 4,3) hydrophobic heptad repeat pattern (hydrophobic residues at positions a and d of the abcdefg heptad), which was responsible for the formation and stability of the coiled coils (Hodges *et al.*, 1972; Sodek *et al.*, 1972). Since then, many new coiled-coil-forming sequences have been reported. However, there is no consensus about the chain length of the peptides or proteins that form two-stranded, α-helical coiled coils. Although the coiled coils observed in the DNA-binding proteins and

† This research is an integral part of the Protein Engineering Network of Centres of Excellence Program supported by the Government of Canada.

* Author to whom correspondence should be addressed.

® Abstract published in *Advance ACS Abstracts,* December 1, 1994.

0006-2960/94/0433-15501$04.50/0

protein kinases vary between 5 and 7 heptads in length (Atkinson *et al.*, 1991; Landschultz *et al.*, 1988; Vinson *et al.*, 1989), such hydrophobic repeats were shown to be continuous throughout the entire 284 residue polypeptide chain of tropomyosin (Sodek *et al.*, 1978; Stone & Smillie, 1978). Actually, coiled coils with as few as 14 residues [GAL4-DNA complex by Marmorstein *et al.* (1992)] and as many as 1086 residues [myosin by McLachlan and Karn (1982)] have been detected. Nevertheless, the significant difference between the sequence and peptide length of the coiled coils and those of their microenviroment observed in biological systems made the direct comparison of their formation and stability very difficult. The majority of studies investigating the factors that contribute to the formation and stability of two-stranded α-helical coiled coils utilized a series of synthetic peptides of *de novo* design containing 5−7 hydrophobic heptad repeats (Hodges *et al.*, 1981, 1988, 1990; Monera *et al.*, 1993; Thompson *et al.*, 1993). It was found that a minimum of 28 amino acid residues was required to form a stable two-stranded, α-helical coiled coil based on the heptad sequence Lys-Ile-Glu-Ala-Leu-Glu-Gly (Lau *et al.*, 1984). However, it is not clear whether this 4-heptad requirement is dependent on the sequence of the hydrophobic repeat. No systematic investigation to date has been concerned with how the chain length of the peptide affects its dimerization ability to form a coiled coil, or with what the stability of the resulting peptide would be. Certainly, a study dedicated to such effects of peptide length should be very useful for designing functional proteins.

In this investigation, our goal is to determine the minimum polypeptide chain length required to form a stable two-stranded dimerization motif based on the heptad sequence of Glu-Ile-Glu-Ala-Leu-Lys-Ala, where the sequence was chosen to maximize hydrophobic and intra- and interchain ionic interactions, along with the high α-helical propensity of the amino acids. This was done by progressively adding one α-helical turn to the peptide chain in order to increase the hydrophobic interactions between the two polypeptide chains.

MATERIALS AND METHODS

Peptide Synthesis and Purification. All peptides were synthesized using the general procedure for solid-phase synthesis described previously (Hodges *et al.*, 1988). Peptide synthesis was carried out on an Applied Biosystems peptide synthesizer Model 430A (Foster City, CA) using the copolymer poly(styrene−1% divinylbenzene)benzhydrylamine hydrochloride resin (0.92 mmol of NH_2/g). After the N-terminus was acetylated with 25% acetic anhydride/dichloromethane (v/v), the peptides were cleaved from the resin by reaction with hydrogen fluoride (20 mL/g of resin) containing 10% anisole and 2% 1,2-ethanedithiol for 1 h at −4 °C. The crude peptides were extracted with 30% acetic acid and lyophilized. Peptide purification was carried out by HPLC[1] using a semipreparative reversed-phase C18 column (Synchropak RP-P, 250 × 10 mm inner diameter, 6.5 μm particle size, 300 Å pore size, SynChrom, Lafayette, IN). The peptides were eluted with a linear AB gradient (ranging from 0.2% to 2.0% B/min, depending on the retention time of the peptide) at a flow rate of 2 mL/min, where solvent A was 0.05% trifluoroacetic acid in water and solvent B was 0.05% trifluoroacetic acid in acetonitrile. The purity and identity of the peptide in the fractions were verified using a Hewlett-Packard HP1090 HPLC equipped with an analytical reversed-phase C8 column (Zorbax 300SB-C8, 25 cm × 4.6 mm, 5 μm particle size, 300 Å pore size) using a linear AB gradient of 2% B/min (solvents A and B are described earlier in this paper). Fractions were pooled and lyophilized. The purified peptides were homogeneous as determined by analytical reversed-phase HPLC, amino acid analysis, and mass spectrometry.

For amino acid analysis, the purified peptides were hydrolyzed in 6 N HCl containing 0.1% phenol at 160 °C for 1 h in an evacuated tube. HCl was then removed using a Savant SC110 SpeedVac concentrator (Savant Instruments, Farmindale, NY) under reduced pressure. Cysteine and cystine were determined following conversion to cysteic acid by adding 2% (v/v) dimethyl sulfoxide to the hydrolysis medium. Amino acid analysis was performed on a Beckman 6300 postcolumn ninhydrin derivatization analyzer equipped with a sulfonated polystyrene cation exchange column and System Gold v6.01 data analysis software (Beckman, San Ramon, CA). Mass spectrometry was carried out on a BIOION 20 Nordic plasma desorption time-of-flight mass spectrometer.

Oxidized peptides (formation of a disulfide bond between the two monomers) were obtained through air oxidation by stirring a solution of the reduced peptides in buffer containing 100 mM NH_4HCO_3 (pH 8.3) overnight at room temperature. The oxidized peptides were purified by reversed-phased HPLC in the same way as the reduced peptides described earlier except that an analytical Zorbax 300SB C8 column was used. The oxidized peptides were verified by RP-HPLC, amino acid composition analysis, and mass spectrometry.

Circular Dichroism Spectroscopy. Circular dichroism (CD) spectra were recorded on a Jasco J-500C spectropolarimeter (Jasco, Easton, MD) at the temperatures indicated in the Results section. The spectropolarimeter was equipped with a Jasco IF-500II interface connected to an IBM PS/2 Model 30286 computer using Jasco DP-500/PS2 system version 1.33a software. A Lauda water bath (Model RMS, Brinkmann Instruments, Rexdale, ON, Canada) was used to control the temperature of the cell. The spectropolarimeter was calibrated daily with an aqueous solution of recrystallized ammonium camphorsulfonate-*10-d*. The molar ellipticity values at 290.5 and 192 nm were +7910 and −15 820, respectively, indicating a ratio of 2, and the photomultiplier voltage was less than 500 V Ellipticity is reported as the mean residue ellipticity ([θ], in deg·cm²/dmol) and calculated as

$$[\theta] = [\theta]_{obs}(MRW/10lc)$$

where $[\theta]_{obs}$ is the ellipticity measured in millidegrees, MRW is the mean residue molecular weight of the polypeptide (molecular weight divided by the number of amino acid residues), c is the concentration of the sample in milligrams/milliliter, and l is the optical path length of the cell in centimeters. Wavelength scans were performed at discrete temperatures from 5 to 85 °C at a peptide concentration of approximately 200 μM (specific peptide concentrations are indicated in the Results section) in a 0.2 mm CD cell. For each temperature point, CD spectra were obtained by

[1] Abbreviations: RP-HPLC, reversed-phase high-performance liquid chromatography; CD, circular dichroism; Gdn·HCl, guanidine hydrochloride; TFE, 2,2,2-trifluoroethanol.

Peptide	Total Ile, Leu Residues	Sequence
9r	1	Ac-K-A-E-I-E-A-C-K-A-amide
12r	2	Ac-E-A-L-K-A-E-I-E-A-C-K-A-amide
16r	3	Ac-K-A-E-I-E-A-L-K-A-E-I-E-A-C-K-A-amide
19r	4	Ac-E-A-L-K-A-E-I-E-A-L-K-A-E-I-E-A-C-K-A-amide
23r	5	Ac-K-A-E-I-E-A-L-K-A-E-I-E-A-L-K-A-E-I-E-A-C-K-A-amide
26r	6	Ac-E-A-L-K-A-E-I-E-A-L-K-A-E-I-E-A-L-K-A-E-I-E-A-C-K-A-amide
30r	7	Ac-K-A-E-I-E-A-L-K-A-E-I-E-A-L-K-A-E-I-E-A-L-K-A-E-I-E-A-C-K-A-amide
33r	8	Ac-E-A-L-K-A-E-I-E-A-L-K-A-E-I-E-A-L-K-A-E-I-E-A-L-K-A-E-I-E-A-C-K-A-amide
35r	9	Ac-E-I-E-A-L-K-A-E-I-E-A-L-K-A-E-I-E-A-L-K-A-E-I-E-A-L-K-A-E-I-E-A-C-K-A-amide
		g a b c d e f g a b c d e f g a b c d e f g a b c d e f g a b c d e f
		1 6 8 13 15 20 22 27 29 34

FIGURE 1: Amino acid sequences of the synthetic peptides used in this study. The N-terminal amino group of the peptide is acetylated and the C-terminal carboxyl group is amidated. The numbers in the peptide names represent the numbers of amino acid residues in the polypeptides, and r indicates that the peptide is in its reduced form (no disulfide bond between the chains). The hydrophobic (Ile and Leu) residues in positions a and d are boxed. The heptad repeat is denoted by the letters abcdefg.

averaging four wavelength scans obtained by collecting data from 255 to 190 nm at 0.1 nm intervals, at a rate of 20 nm min^{-1}, a response time of 4 s for each point, and a bandwidth of 1 nm. Wavelength scans were corrected for buffer scans taken at 20 °C and normalized for concentration to obtain the mean residue ellipticity. The ellipticities at 222 nm were obtained using the time scan mode of the software. Each point was the average of a minimum of 40 × 1 s measurements with a bandwidth of 1 nm. Time scans were also processed by subtracting buffer scans and normalized for peptide concentration. The limits of error of measurement at 222 nm were ± 500 deg/sample, each sample being run several times. Peptide concentrations were determined by amino acid analysis.

Denaturation Studies. The stock solutions of the polypeptides prepared in benign buffer (50 mM phosphate/100 mM KCl, pH 7.0) were diluted with calculated volumes of 8 M guanidine hydrochloride (Gdn·HCl) dissolved in the same buffer to give the desired final denaturant concentrations. The samples were incubated at room temperature for a minimum of 3 h before their full-range CD spectra or the ellipticities at 222 nm were recorded.

For temperature denaturation studies, the stock peptide solutions were diluted with appropriate volumes of buffer and denaturant (Gdn·HCl). Wavelength and time scans were recorded after 10 min of equilibration of the sample at different temperatures. Ellipticity readings were normalized to the fraction of the peptide folded using the standard equation:

$$f_n = ([\theta] - [\theta]_u)/([\theta]_n - [\theta]_u)$$

where $[\theta]_n$ and $[\theta]_u$ represent the ellipticity values for the fully folded and fully unfolded species, respectively. $[\theta]$ is the observed ellipticity at 222 nm at any denaturant concentration or temperature.

Molecular Weight Determination. The molecular weights of the peptides in benign buffer were determined by size-exclusion chromatography and sedimentation equilibrium experiments. Size-exclusion chromatography was carried out on a Superdex 75 size-exclusion column (Pharmacia LKB Biotechnology, Uppsala, Sweden) attached to a Hewlett-Packard Model 1090 liquid chromatography system. The peptides were eluted from the column with benign buffer at a flow rate of 0.2 mL/min at room temperature. Sedimentation equilibrium experiments were carried out in a Beckman Model E analytical ultracentrifuge equipped with electronic speed control and RTIC temperature control, using Rayleigh interference optics. An ANH titanium rotor and double sector charcoal-filled Epon cells were used for all runs. Measurements of photographic plates were performed on a Nikon Model 6 microcomparator at a magnification of 50×. Samples were dialyzed against benign buffer for a minimum of 48 h at 4 °C before sedimentation equilibrium runs were carried out. Sedimentation equilibrium experiments were performed for a minimum of 36−48 h prior to taking equilibrium photographs. For reduced peptides, 15 mM dithiothreitol (DTT) was added to the buffer to prevent the formation of an interchain disulfide bond. For peptide 23ox (the oxidized form of 23r), the experiment was run at 48 000 rpm with a peptide concentration of 1.58 mg/mL.

RESULTS AND DISCUSSION

Design of the Peptides. To investigate the effect of the peptide chain length on the formation of two-stranded dimers or coiled coils and protein stability, a series of peptides containing 9−35 amino acid residues was synthesized. Following a consistent heptad repeat, one hydrophobic residue (leucine or isoleucine) was systematically added to the hydrophobic core of the peptide progressively in order to obtain maximum stability. Figure 1 shows the amino acid sequences of the polypeptides used in the present study. The possible formation of a two-stranded coiled coil by peptide 23r, where the two identical 23 residue polypeptide chains interact in a parallel and an in-register manner, is shown schematically in Figure 2. The N-termini were acetylated and the resins were chosen to yield peptides with C-terminal amides upon cleavage in order to avoid the introduction of charges and possible unfavorable interactions with the

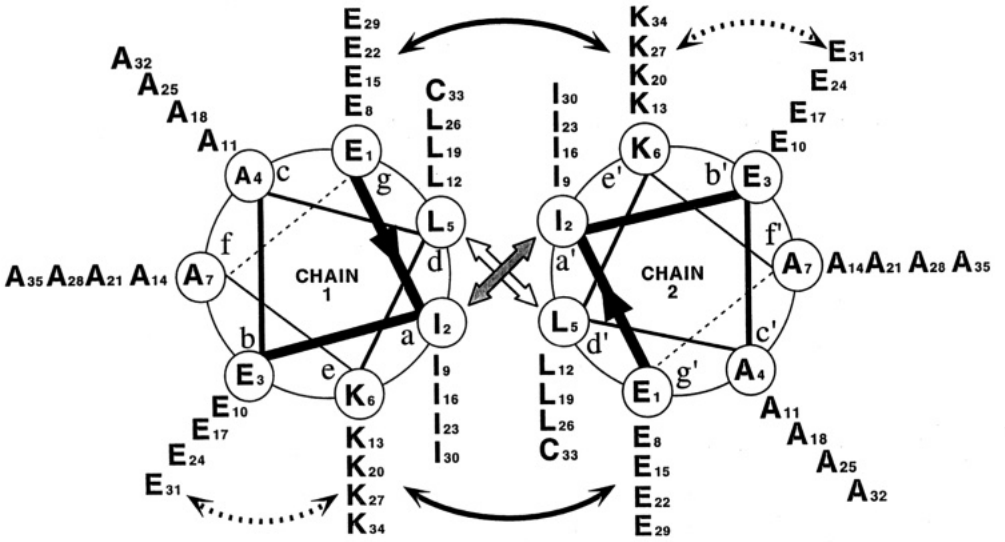

FIGURE 2: Schematic representation of two-stranded, α-helical coiled coils formed by the dimerization of 35r. The chains are in register and parallel. The letters a to g and a′ to g′ designate the positions in the heptad repeat. The number following the capital letter indicates the position of that amino acid residue in the peptide sequence starting from the N-terminal end. The hydrophobic residues at a and a′ and d and d′ interact and are mainly responsible for the formation and stabilization of the coiled coil. Electrostatic attractions could occur between b and e (b′ and e′), that is *i,i*+3 intrachain interactions, or e and b (e′ and b′), that is, *i,i*+4 intrachain interactions (dashed arrows). Interchain interactions *i,i*′+5 (electrostatic attractions) (g−e′ or g′−e) are indicated by the solid arrows.

α-helix dipole (Shoemaker *et al.*, 1987; Fairman *et al.*, 1989; Dasgupta & Bell, 1993).

In the design of these peptides, several features were incorporated that are known to stabilize α-helices and coiled coils. For particular positions (f and c, Figure 2) the amino acid residue, alanine, was selected because of its high intrinsic helical propensity (Chou & Fasman, 1978; Lyu *et al.*, 1990; O'Neil & DeGrado, 1990; Chakrabartty *et al.*, 1994; Zhou *et al.*, 1994a). The five residues (Ala, Glu, Ile, Lys, and Leu) used in our sequence are actually the most frequently found amino acids in the heptad repeat of native proteins (Cohen & Parry, 1990). Secondary structure predictions using the methods of Chou and Fasman (1978) and Eisenberg *et al.* (1984) suggest that all of the amino acid residues used in our study should adopt an α-helical conformation.

It is generally believed that hydrophobic interactions are the major forces involved in initiating protein folding and stabilizing the overall configuration of proteins (Kellis *et al.*, 1988, 1989; Dill, 1990; Eriksson *et al.*, 1992). Both empirical calculations and experimental evidence reveal that hydrophobic packing and hydrophobicity within the interface are the major forces contributing to the overall stability of a coiled coil (Krystek *et al.*, 1991; Hodges *et al.*, 1990; Zhou *et al.*, 1992b,c; Zhu *et al.*, 1993). Analysis of coiled coil/leucine zipper sequences have shown that generally β-branched amino acids are preferred at a positions, while Leu residues are usually found at d positions (Cohen & Parry, 1990; McKnight, 1991; Hu & Sauer, 1992). Mutation of leucine to valine or isoleucine in synthetic coiled coils also indicated a preference for β-branched amino acids at a and the conservation of leucine residues at d with regard protein stability (Zhu *et al.*, 1993). Isoleucine and leucine therefore were chosen as the hydrophobic amino acids and placed at positions a and d of the heptad, respectively.

As well, the hydrophilic charged amino acids lysine and glutamic acid were chosen and placed at positions of the peptide so that intramolecular electrostatic attractions were incorporated. As shown in Figures 1 and 2, the glutamate/lysine ion pairs are located in the *i* and *i*+3 (b−e) or *i* and *i*+4 positions (e−b) along the sequence, which could provide additional stability to the α-helical structure by side-chain electrostatic interactions (Marqusee & Baldwin, 1987; Merutka & Stellwagen, 1991; Scholtz & Baldwin, 1992; Zhou *et al.*, 1993). Marqusee and Baldwin (1987) reported that intrachain *i, i*+4 ionic interactions provide greater stability to α-helices than do *i,i*+3 interactions. Although the bulk of the interaction at the interface of the coiled coils is hydrophobic, interchain electrostatic interactions between the two polypeptide chains, such as those between Glu and Lys in the e−g′ and e′−g positions (Hodges *et al.*, 1988; Talbot & Hodges, 1982), provide the necessary additional free energy of stabilization (Monera *et al.*, 1993; Thompson *et al.*, 1993; Zhou *et al.*, 1994b). In addition, the strategic positioning of the Lys and Glu residues increases the specificity to form either parallel or antiparallel coiled coils (Monera *et al.*, 1994a).

Formation of Coiled Coils. The solution conformations of the synthetic peptides were studied by ultraviolet CD spectroscopic methods under various conditions. Typical CD spectra of samples of varying chain lengths at concentrations of 210 ± 15 μM in aqueous solution and in the presence of the α-helix inducing solvent (TFE) are shown in Figure 3. The CD spectral features and the absolute mean residue ellipticities were significantly affected by the chain length of the peptide. Quantitative assessment of the secondary structure content of the spectra was made according to the method of Chan *et al.* (1974). The results are summarized in Table 1. In the presence of 50% TFE, all nine peptides, ranging from 9 to 35 residues in length, displayed CD spectra of significant α-helix content. However, in aqueous solution (benign buffer 50 mM phosphate/0.1 M KCl, pH 7.0), the spectrum of peptide 9r (Figure 3) shows features typical of a sample containing both turns and random coil (Chen *et al.*, 1972). Similar results were observed for peptide 12r. In contrast, peptide 19r showed clear indications of the presence of helix in the sample, with a subminimum in the 220 nm region and a minimum at 205 nm (Figure 3).

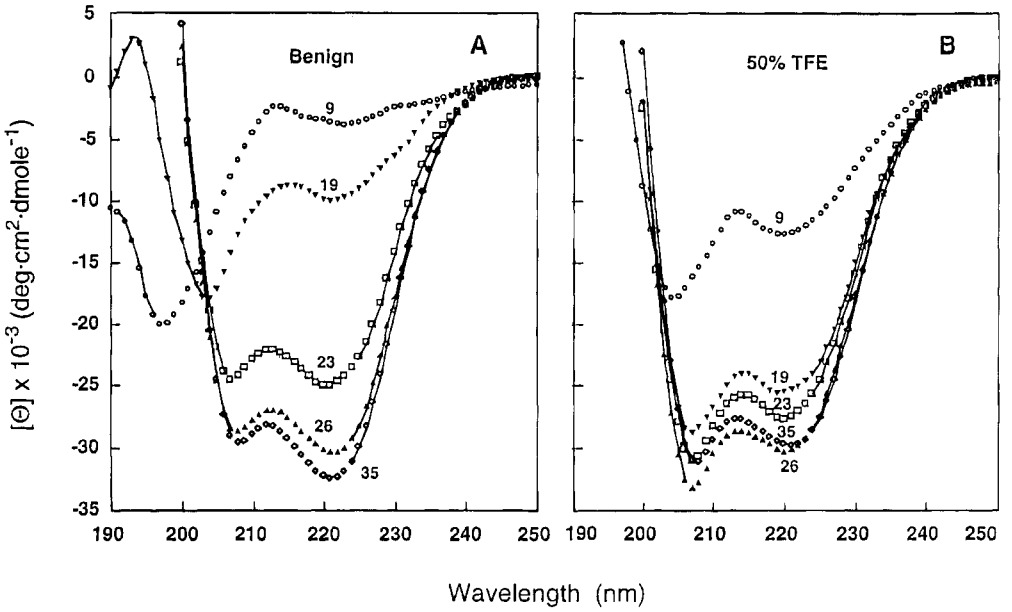

FIGURE 3: Circular dichroism spectra of peptide analogs of various chain lengths in the presence (B) and absence (A) of the α-helix-inducing solvent, trifluoroethanol (TFE). The wavelength scans were performed in benign medium at 20 °C. Circles denote the peptide 9r at 210 μM; triangle (down), peptide 19r at 206 μM; squares, peptide 23r at 210 μM; triangle (up), peptide 26r at 202 μM; and diamonds represent the CD spectrum of peptide 35r at 227 μM.

Table 1: Chain Length Dependence of the Ellipticity and Helix Content of Peptide Analogs

		$[\theta]_{222}$ (deg/cm²/dmol)[a]						helix content (%)[d]	
peptide	[peptide] (μM)	benign	change[b]	50% TFE	change[b]	$\Delta[\theta]_{222}$[c]	calculated 100% helix value	benign	50% TFE
9r	216	−3700		−12340		8640	−27011	13.7	45.7
12r	210	−3600	+100	−20200	−7860	16600	−29608	12.1	68.1
16r	194	−6400	−2800	−24300	−4100	19900	−31556	20.3	74.8
19r	198	−9940	−3540	−25220	−920	15280	−32478	30.6	77.7
23r	206	−24730	−14790	−26940	−1720	2210	−33334	74.2	80.8
26r	202	−30300	−5570	−29720	−2780	580	−33803	89.6	87.9
30r	207	−32250	−1950	−32550	−2830	300	−34283	94.1	94.9
33r	220	−32420	−170	−32260	+290	160	−34566	93.4	93.3
35r	227	−32370	+50	−31680	+580	690	−34728	93.2	91.2

[a] Calculated molar ellipticity of the peptide at 222 nm. [b] Ellipticity change compared with that of the previous peptide containing one less hydrophobic residue (leucine or isoleucine) in the hydrophobic core of the peptide. [c] $\Delta[\theta]_{222}$ is the difference between the ellipticity at 222 nm in benign buffer and that in 50% TFE: $\Delta[\theta]_{222} = [\theta]_{222}$(benign) − $[\theta]_{222}$(50% TFE). [d] The predicted molar ellipticity (X_H^n) is based on theoretical values as described by Chen *et al.* (1974) using a $[\theta]_{222}$ value of −37 400 deg·cm² dmol⁻¹ for a helix of infinite length (X_H^∞). The equation used is $X_H^n = X_H^\infty (1 - k/n)$, where n is the number of residues/helix and k is a wavelength-dependent constant (2.5 at 222 nm).

However, the spectrum has low negative ellipticity, signifying that the α-helix is not the predominant structural component (Table 1). Introduction of an additional helical turn to peptide 19r significantly changed the CD spectrum and the α-helix content of the peptide. Peptides containing 23 or more residues all showed CD spectra typical of α-helical proteins with two minima at 222 and 207 nm (Figure 3) (Chen *et al.*, 1972; Gans *et al.*, 1991). The highly negative molar ellipticity values indicate high helical content (Table 1). These long peptides are essentially 100% helical in benign medium compared with those when 50% TFE is present. Overall, peptides 9r−35r exhibited progressively more negative intensity in the α-helix region, demonstrating that the contribution of this component increases with chain length (Table 1). For short peptides (19 residues or less), although the molar ellipticity becomes more negative as the peptide chain advances in length, the helix contents are generally low. For peptides of 26 or more residues, an increase in peptide length also has little effect on the peptide ellipticity or the helix content. The most significant change was observed when the peptide length was increased from 19 to 23 residues, with an increase in both the molar ellipticity at 222 nm and the helix content by 240%.

In aqueous solution, the molar ellipticity of the peptide was generally concentration dependent, and an aggregation-induced increase in helicity with increasing peptide concentration was detected (Figure 4A). For peptides with 23 or more amino acids, the helicity reached a plateau at 60−70 μM peptide with high negative values of $[\theta]_{222}$. In contrast, the ellipticity of short peptides (19 residues or less) was very low, even at peptide concentrations as high as 3 mM, implying a low content of α-helix. The relationship between ellipticity and peptide chain length is shown in Figure 4B. It is clear that, over the concentration range tested, the nine peptides used in the present study can be categorized into two groups. Although the mean molar ellipticity at 222 nm becomes more negative as the peptide length increases, category A peptides (19 or less residues) show low α-helical content compared with category B peptides (23 residues or more), which contain predominantly α-helix. A likely explanation of this concentration dependence behavior with regard to the molar ellipticity is attributed to the formation

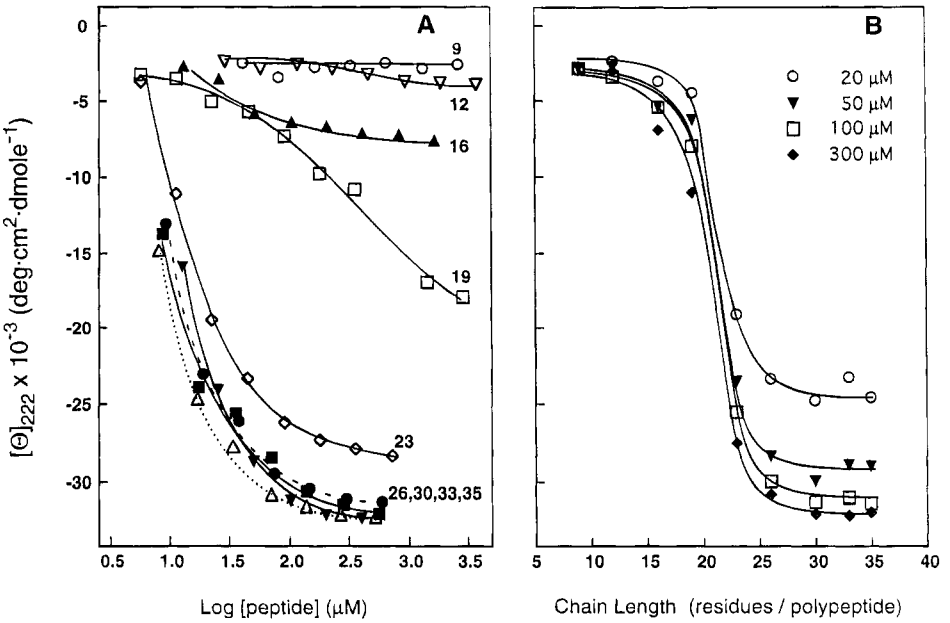

FIGURE 4: (A) Effect of peptide concentration on the ellipticity at 222 nm for peptides of varying chain lengths: open circles, 9r; open triangles (down), 12r; closed triangles (up), 16r; open squares, 19r; open diamonds 23r; closed circles, 26r; open triangles (up); 30r; closed triangles (down); 33r; closed squares, 35r. (B) Ellipticity at 222 nm for peptides of various chain lengths. Data were taken from part A.

of two-stranded, α-helical coiled coils. When the concentration of the peptide is increased, the equilibrium between monomeric peptide (in the form of random coil) and coiled-coil dimer is shifted toward the formation of the coiled-coil dimer, which increases the α-helical content of the peptide (Zhou *et al.*, 1992a).

TFE can increase the helicity of single-stranded peptides and has been widely used as an α-helix-inducing cosolvent (Goodman & Listowsky, 1962; Lau *et al.*, 1984; Sonnichsen *et al.*, 1992). The molar ellipticity at 222 nm of peptide as a function of TFE concentration is illustrated in Figure 5A. As the polarity of the medium decreases, the helicity of short peptides (category A) increases substantially, indicating that the peptides are induced to fold into significantly more helical conformations by TFE. Nevertheless, the ellipticity of peptides in category B changed less than 10% upon the addition of TFE, exhibiting their nearly fully helix content even without TFE (also Table 1). More revealing is the observation that the ellipticity ratio of $[\theta]_{222}$ to $[\theta]_{208}$ decreased with increasing TFE concentration for category B peptides (Figure 5B). The ratio decreased steadily from 1.02−1.07 to 0.87−0.93 over the range 0−70% TFE. This decrease in the ellipticity ratio has also been observed with other synthetic peptides accompanying the transition from two-stranded, α-helical coiled coils to single-stranded α-helices (Lau *et al.*, 1984; Engel *et al.*, 1991; Zhu *et al.*, 1992; Monera *et al.*, 1993). The values of the molar ellipticity ratio for category B peptides, in benign medium and in the presence of TFE, obtained in this study are consistent with those reported for two-stranded coiled coils (aqueous solution) and for a single-stranded α-helix in TFE (Lau *et al.*, 1984). Upon comparing the CD spectra in benign medium and in the presence of 50% TFE (Figure 3), it was found that although the helical content was not affected significantly, as suggested by the comparable 222 nm values in the two media, the 208 nm band has now increased appreciably in negative ellipticity by the addition of TFE, indicating the transition from a two-stranded, α-helical coiled coil to a single-stranded helix (Cooper &d Woody, 1990). Therefore, the results of the TFE titration experiments indicate that TFE converts the coiled coils formed by long peptides (23 residues or more) to single-stranded α-helical structures by disrupting the hydrophobic interactions between the two chains.

Size-exclusion chromatography and sedimentation equilibrium experiments indicated that the 23r peptide has essentially the same molecular weight (4600−5000) as that of the oxidized form of the peptide, indicating the dimerization of the reduced peptide in aqueous solution (data not shown). The results of this study fulfill the criteria used to establish the existence of two-stranded, α-helical coiled coils (Zhu *et al.*, 1993). First, the CD spectra of category B peptides all showed the double minima at 207 and 222 nm with high negative ellipticity values, which characterizes a fully formed α-helical structure. Second, the ellipticity of the reduced peptides exhibited concentration dependence due to the monomer−dimer equilibrium. Third, the reduced peptide showed the same apparent molecular weight as that of the oxidized peptide, and finally, in benign medium, category B peptides had an ellipticity ratio ($[\theta]_{222}/[\theta]_{208}$) of 1.04, which is consistent with the value previously reported for two-stranded coiled coils (Lau *et al.*, 1984; Hodges *et al.*, 1988; Zhou *et al.*, 1992b; Monera *et al.*, 1993). Therefore, it is reasonable to conclude that two-stranded, α-helical coiled coils are formed by peptides 23r, 26r, 30r, 33r, and 35r in aqueous solution, in contrast to the short peptides in category A where no coiled coils are detected.

The molar ellipticities for peptides of varying chain lengths were compared with the predicted values (Figure 6) according to the method of Chen *et al.* (1974). The observed ellipticities for peptides of varying chain length were different from the predicted values, whether in benign solution or in 50% TFE. This deviation was also observed in a previous study from our laboratory (Lau *et al.*, 1984). The end effects in short peptides should be maximal compared to the same chain length in proteins, because the ends of the helices in proteins are conformationally restricted by the tertiary structure of the remaining polypeptide chains. The formation

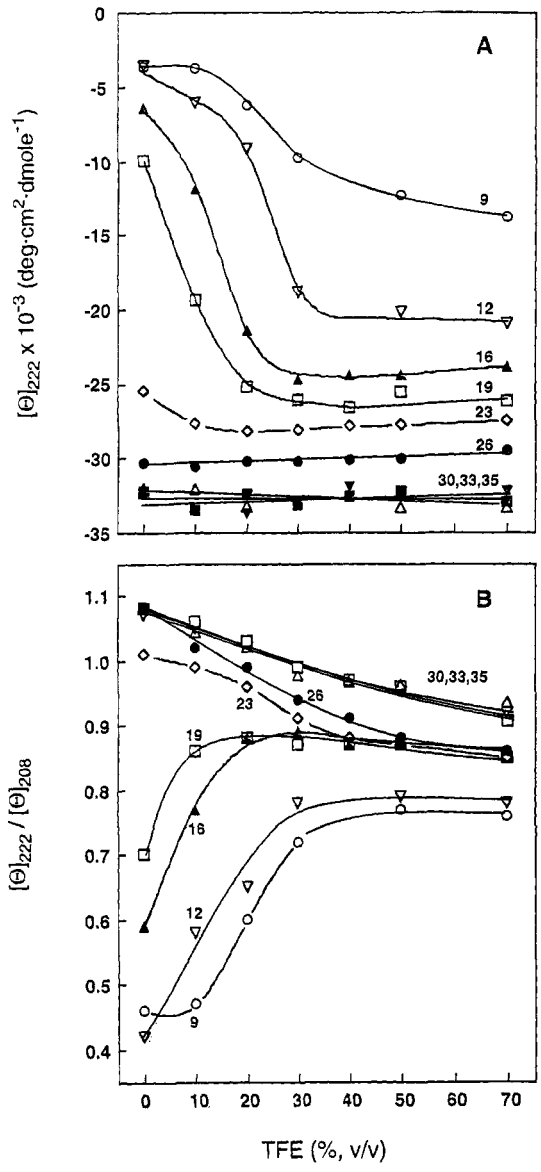

FIGURE 5: Influence of the α-helix-inducing solvent (TFE) on peptides of different chain lengths: (A) ellipticities of peptides at 222 nm; (B) ratio of ellipticities at 222 to 208 nm. Ellipticity values were taken from the CD spectra ranging from 255 to 190 nm. The wavelength scans were performed at 20 °C in benign buffer containing the indicated concentrations of TFE. Peptide concentrations were held at 210 ± 15 μM. Symbols are the same as for part A.

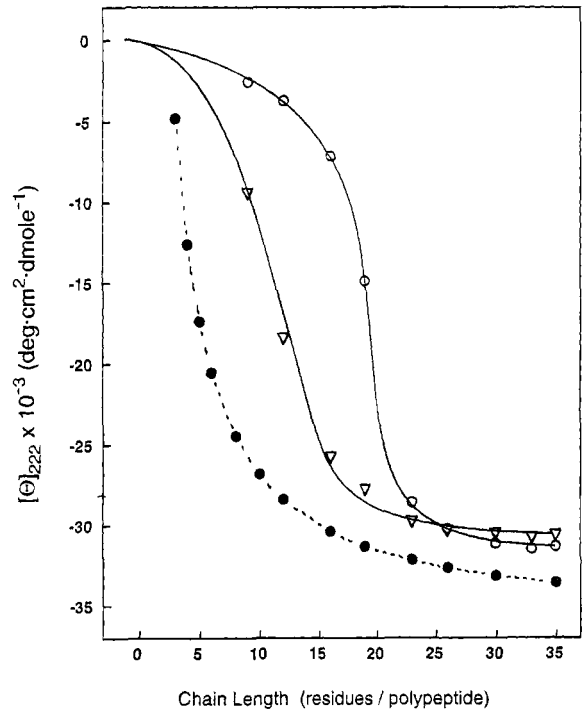

FIGURE 6: Comparison of observed molar ellipticity and predicated molar ellipticity at 222 nm versus chain length. The predicted ellipticity is based on theoretical values as described by Chen *et al.* (1974). The observed values are those of peptides 9r−35r at a peptide concentration of 210 ± 15 μM. The open circles are the observed ellipticities in benign buffer, the open triangles are those in the presence of 50% TFE, and the closed circles are the predicted molar ellipticities.

of a two-stranded, α-helical coiled coil provides a protein-like scenario. Thus, it is not surprising that the observed ellipticities for peptides that form dimeric coiled coils (more than 23 residues) are very close to the predicted values, whereas the ellipticities of short peptides that do not form coiled coils deviate substantially (Figure 6). Our result of a minimum length requirement (23 residues) for the formation of a two-stranded coiled coil is in agreement with the recent report that the α-helical coiled coils have a mean length of 28 ± 9 residues, as deduced by crystal structure studies (Dohlman *et al.*, 1993).

Stability of Proteins. In accordance with the general view that hydrophobic interaction is the major stabilizing force in proteins and synthetic coiled coils, we would expect to find an increase in coiled-coil stability with an increase in the number of these interactions as the peptide chain increases in length. The stability of the coiled coils was determined by Gdn·HCl and thermal denaturation experiments, where the changes in ellipticity at 222 nm were monitored by CD. $[Gdn{\cdot}HCl]_{50}$ values are widely used to estimate the relative strength of hydrophobic interactions when comparing different proteins (Monera *et al.*, 1994b). Figure 7A shows that the $[Gdn{\cdot}HCl]_{50}$ values of the peptides varied with chain length. Since the stability is affected by peptide concentration (Zhou *et al.*, 1992a,b), a similar peptide concentration was used throughout. The concentration was chosen so that two-stranded, α-helical coiled coils could be formed in benign medium for peptides of 23 or more residues. The normalized denaturation curves, in which the molar ellipticity of peptides in 50% TFE solution was represented as 100% helical, also exhibited similar trends (Figure 7B). As expected, the $[Gdn{\cdot}HCl]_{50}$ of the peptide markedly depends on the length of the peptide. Peptides 23r−35r have reasonable stabilities that are in agreement with those from previous studies (Hodges *et al.*, 1981; Lau *et al.*, 1984). Peptide 23r required 3 M Gdn·HCl for 50% unfolding, whereas peptide 35r was so stable that only 20% of the peptide was denatured at 7.5 M Gdn·HCl. Gdn·HCl masks electrostatic interactions and at higher concentrations promotes denaturation (Monera *et al.*, 1993, 1994). From peptide 23r to 33r, one hydrophobic residue was added to the hydrophobic interface of the coiled coil. If these hydrophobic interactions contribute equally to the stability of coiled coils, the $[Gdn{\cdot}HCl]_{50}$ values should increase by the same amount when each helical turn (hydrophobic interaction) is added to the sequence. In Figure 7C it is noted that the value of $[Gdn{\cdot}HCl]_{50}$ increased by 1.7, 2.1, and 0.6 M for the first (from 23r to 26r), second (26r−30r), and third added helical turns (30r −33r), respectively. When this chain

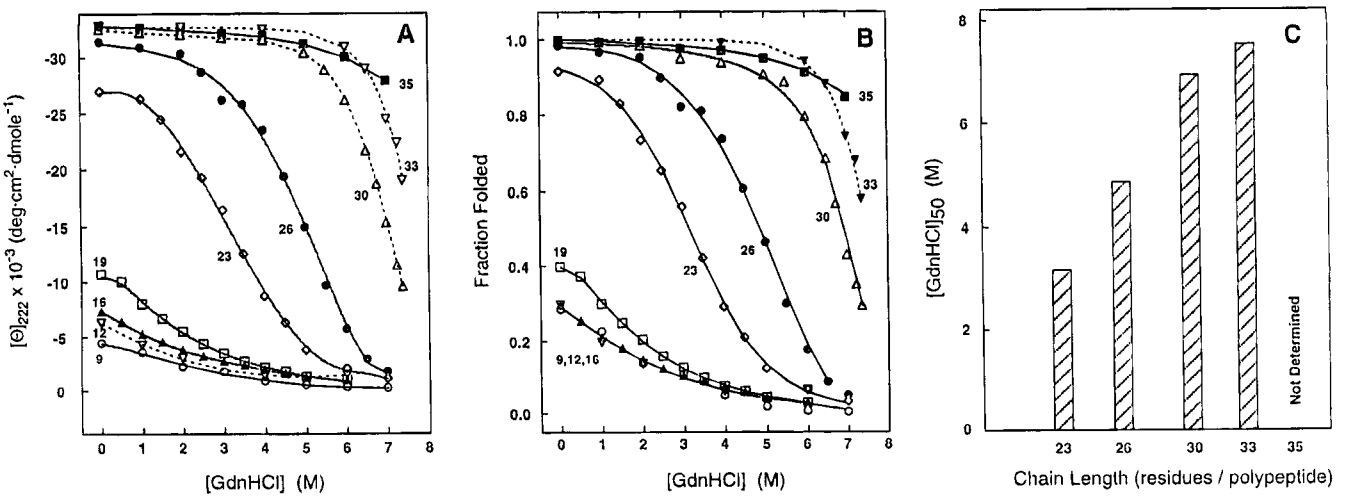

FIGURE 7: Gdn·HCl denaturation profiles of the reduced synthetic peptides in benign medium: (A) Effect of the denaturant on the ellipticitiicites of the peptides at 222 nm; (B) Normalized denaturation curves. Curves were calculated from the results in part A, as described in the text. The ellipticity of peptide in the presence of 50% TFE was taken as that of the fully folded species. Symbols have the same meanings as in Figure 4A. (C) Stability of peptides of varying chain lengths. $[Gdn{\cdot}HCl]_{50}$ represents the concentration of denaturant at which 50% of the peptide is unfolded.

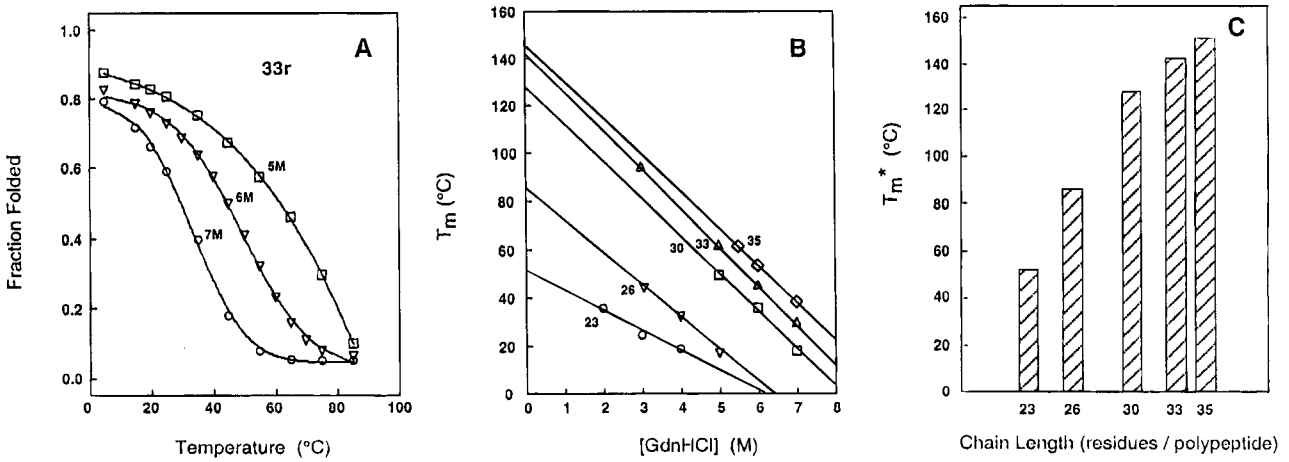

FIGURE 8: (A) Thermal melting profiles of peptide 33r in the presence of 5 (squares), 6 (triangles), and 7 (circles) Gdn·HCl. Curves were calculated on the basis of the ellipticity at 222 nm at different temperatures. The ellipticity at 5 °C in the presence of 50% TFE was used for the 100% folded peptide. (B) Dependence of the thermal stability of synthetic peptides of different chain lengths on the concentration of denaturant: circles, peptide 23r; triangles (down), peptide 26r; squares, peptide 30r; triangles (up), peptide 33r; diamonds, peptide 35r. T_m is the temperature at which 50% of the peptide is unfolded in the presence of Gdn·HCl. (C) Thermal stability of peptides in aqueous solution without denaturant. T_m* is the temperature at which 50% of the peptide is unfolded in 50 mM phosphate/0.1 M NaCl, pH 7.0. T_m* is obtained by extrapolating the curves in part B.

length effect was normalized with respect to the stability of the coiled coils, the numbers become 0.57, 0.51, and 0.20 M/hydrophobic residue. Clearly, as the chain length of the peptide increases, with the consequent increase in the number of hydrophobic interactions, the stability the of coiled coils increases but in a nonlinear form. After five heptad repeats, the increase in stability with further increases in chain length is probably minimal.

The stability of coiled coils of varying lengths was also studied by comparing their temperature melting curves. Curves corresponding to a smooth, cooperative transition were obtained by plotting the observed molar ellipticity at 222 nm versus the temperature. Since 100% unfolding was not observed for these peptides under the experimental conditions, different amounts of denaturant (Gdn·HCl) were included in thermal unfolding experiments. Figure 8A demonstrates the effect of elevated temperature, under benign conditions and in the presence of denaturant (Gdn·HCl), on the molar ellipticity at 222 nm of peptide 33r. The melting curves are shifted to the left, with lower T_m values, which is the temperature at which 50% of the α-helical structure is lost using the helical content at 5 °C in the presence of 50% TFE and no denaturant as 100%. Because raising the temperature and adding Gdn·HCl both disrupt hydrophobic interactions, the destabilization effect is expected to be additive. As shown in Figure 7A, the melting curves were shifted toward low temperature with increasing Gdn·HCl concentration. Similar results were reported when urea was used as the denaturant (Lau *et al.*, 1984). For all peptides capable of forming two-stranded, α-helical coiled coils, a linear relationship was found between the melting temperature of the peptide and the denaturant concentration (Figure 8B). In order to compare the thermal stability of the peptides, it is necessary to obtain the T_m in the absence of Gdn·HCl (T_m*, T_m in the absence of denaturant). The effect of chain length on the thermal stability of coiled coils is illustrated in Figure 8C. Consistent with the results of the Gdn·HCl denaturation experiments, an increased thermal

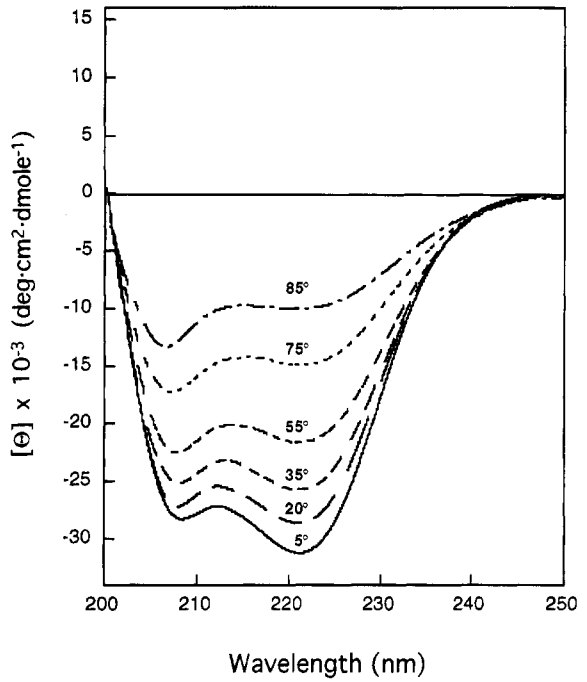

FIGURE 9: Temperature dependence of the CD spectra of peptide 23r in benign buffer: solid line, CD spectra at 5 °C; long dash, 20 °C; medium dash, 35 °C; dot, 55 °C; short dash, 75 °C; dash-dot, 85 °C. Peptide concentration was 70 μM.

stability was observed with an increase in chain length; however, but in a nonlinear cooperative manner, T_m* was increased by 34 °C when the peptide length was increased from 23 to 26 residues. An even larger shift was observed (42 °C) when the peptide was increased to 30r from 26r. However, addition of another hydrophobic interaction pair to 30r made the T_m* only 14 °C higher, compared with a 9 °C change between peptides 33r and 35r. As chain length increases, the importance of hydrophobic interactions with regard to stability is decreased significantly.

The thermal folding/unfolding transition was found to be reversible, as indicated by the recovery of the CD spectra upon cooling (data not shown). To understand the nature of the unfolding of coiled coils, the CD spectrum in the 190–250 nm wavelength range of peptide 23r was measured as a function of temperature. Figure 9 shows the family of temperature curves obtained at a peptide concentration of 70 μM. The measured spectra, especially those at high temperature, are well represented by the population-weighted superimposition of the characteristic spectra for α-helix and random coil conformations (Chen *et al.*, 1972). The existence of an isodichroic point in the vicinity of 203 nm in these spectra indicates that the thermal unfolding proceeds by a two-state mechanism: one state representing the native, folded coiled coil and the other a set of states loosely corresponding to a random coil (Engel *et al.*, 1991; Gans *et al.*, 1991; Thompson *et al.*, 1993; Moser, 1992), The smooth transition curves observed in the denaturation studies (Figures 7A and 8A) also indicate that there are no transition intermediates when the coiled coils are thermally unfolded or denatured by Gdn·HCl.

In conclusion, the results of this study clearly demonstrate that the formation and stability of synthetic coiled coils are influenced significantly by the chain length of the peptide. By using a heptad sequence of Glu-Ile-Glu-Ala-Leu-Lys-Ala, it was found that a minimum of three heptad repeats was required to form a stable two-stranded, α-helical coiled coil, and it appears to be optimal after five heptad repeats.

ACKNOWLEDGMENT

We thank Paul Semchuk for peptide synthesis and purification, Bob Luty and Leslie Hicks for performing the CD and sedimentation equilibrium experiments, respectively, and Terri Keown for carrying out the amino acid analysis. We are also indebted to Dr. O. Monera for helpful discussions.

REFERENCES

Adamson, J. G., Zhou, N. E., & Hodges, R. S. (1993) *Curr. Biol. 4*, 428–437.

Atkinson, R. A., Saudek, V., Huggins, J. P., & Pelton, J. T. (1991) *Biochemistry 30*, 9387–9395.

Chakrabarty, A., Kortemme, T., & Baldwin, R. L. (1994) *Protein Sci. 3*, 843–852.

Chen, Y.-H., Yang, J. T., & Martinez, H. M. (1972) *Biochemistry 11*, 4120–4131.

Chen, Y.-H., Yang, J. T., & Chau, K. H. (1974) *Biochemistry 13*, 3350–3359.

Chou, P. Y., & Fasman, G. D. (1978) *Annu. Rev. Biochem. 47*, 251–276.

Cohen, C., & Parry, D. A. D. (1986) *Trends Biochem. Sci. 11*, 245–248.

Cohen, C., & Parry, D. A. D. (1990) *Proteins 7*, 1–15.

Cooper, T. M., & Woody, R. W. (1990) *Biopolymers 30*, 657–676.

Crick, F. H. C. (1953) *Acta Crystallogr. 6*, *689*–697.

Dasgupta, S., & Bell, J. A. (1993) *Int. J. Pept. Protein Res. 41*, 499–511.

Dill, K. A. (1990) *Biochemistry 29*, 7133–7155.

Dohlman, J. G., Lupas, A., & Carson, M. (1993) *Biochem. Biophys. Res. Commun. 195*, 686–696.

Eisenberg, D., Weiss, R. M., & Terwilliger, T. C. (1984) *Proc. Natl. Acad. Sci. U.S.A. 81*, 140–144.

Engel, M., Williams, R. W., & Erickson B. W. (1991) *Biochemistry 30*, 3161–3169.

Enser, M., Bloomberg, G. B., Brock, C., & Clark, D. C. (1990) *Int. J. Macromol. 12*, 118–124.

Eriksson, A. E., Baase, W. A., Zhang, X.-J., Heinz, D. W., Blaber, M., Baldwin, E. P., & Matthews, B. W. (1992) *Science 255*, 178–183.

Fairman, R., Shoemaker, K. R., York, E. J., Stewark, J. M., & Baldwin, R. L. (1989) *Proteins 5*, 1–7.

Gans, P. L., Lyu, P. C., Manning, M. C., Woody, R. W., & Kallenbach, N. R. (1991) *Biopolymers 31*, 1605–1614.

Goodman, M., & Listowsky, I. (1962) *J. Am. Chem. Soc. 84*, 3770–3771.

Hodges, R. S. (1972) *Cold Spring Harbor Symp. Quant. Biol. 37*, 299–310.

Hodges, R. S. (1992) *Curr. Biol. 2*, 122–124.

Hodges, R. S., Saund, A. K., Chong, P. C. S., St.-Pierre, S. A., & Reid, R. E. (1981) *J. Biol. Chem. 256*, 1214–1224.

Hodges, R. S., Semchuk, P. D., Taneja, A. K., Kay, C. M., Parker, J. M. R., & Mant, C. T. (1988) *Pept. Res. 1*, 19–30.

Hodges, R. S., Zhou, N. E., Kay, C. M., & Semchuk, P. D. (1990) *Pept. Res. 3*, 123–137.

Hu, J. C., & Sauer, R. T. (1992) *Nucleic Acids Mol. Biol. 6*, 82–101.

Kellis, J. T., Jr., Nyberg, K., & Fersht, A. R. (1988) *Biochemistry 28*, 4914–4922.

Kellis, J. T., Jr., Nyberg, K., Sali, D., & Fersht, A. R. (1989) *Nature 333*, 784−786.
Krystek, S. R., Jr., Bruccoleri, R. E., & Novotny, J. (1991) *Int. J. Pept. Protein Res. 38*, 229−236.
Landschultz, W. H., Johnson, P. J., & McKnight, S. L. (1988) *Science 240*, 1759−1764.
Lau, S. Y. M., Taneja, A. K., & Hodges, R. S. (1984) *J. Biol. Chem. 259*, 13253−13261.
Lee, H., Faraggi, M., & Klapper, M. H. (1992) *Biochim. Biophys. Acta 1159*, 286−294.
Lupas, A., van Dyke, M., & Stock, J. (1991) *Science 252*, 1162−1164.
Lyu, P. C., Liff, M. I., Marky, L. A., & Kallenbach, N. R. (1990) *Science 250*, 669−673.
Marmorstein, R., Carey, M., Ptashne, M., & Harrison, S. C. (1992) *Nature 356*, 408−414.
Marqusee, S., & Baldwin, R. L. (1987) *Proc. Natl. Acad. Sci. U.S.A. 84*, 8898−8902.
McKnight, S. L. (1991) *Sci. Am. 264* (April), 54−64.
McLachlan, A. D., & Karn, J. (1982) *Nature 299*, 226−231.
Merutka, G., & Stellwagen, E. (1991) *Biochemistry 30*, 1591−1594.
Monera, O. D., Zhou, N. E., Kay, C. M., & Hodges, R. S. (1993) *J. Biol. Chem. 268*, 19218−19227.
Monera, O. D., Kay, C. M., & Hodges, R. S. (1994a) *Biochemistry 33*, 3862−3871.
Monera, O. D., Kay, C. M., & Hodges, R. S. (1994b) *Protein Sci.* (in press).
Moser, R. (1992) *Protein Eng. 5*, 323−331.
O'Neil, K. T., & DeGrado, W. F. (1990) *Science 250*, 646−651.
O'Shea, E. K., Klemm, J. D., Kim, P. S., & Alber, T. (1991) *Science 254*, 539−544.
Scholtz, J. M., & Baldwin, R. L. (1992) *Annu. Rev. Biophys. Biomol. Struct. 21*, 95−118.
Shoemaker, K. R., Kim, P. S., York, E. J., Stewart, J. M., & Baldwin, R. L. (1987) *Nature 326*, 563−567.
Sodek, J., Hodges, R. S., Smillie, L B., & Jurasek, L. (1972) *Proc. Natl. Acad. Sci. U.S.A. 69*, 3800−3804.
Sodek, J., Hodges, R. S., & Smillie, L. B. (1978) *J. Biol. Chem. 253*, 1129−1136.
Sonnichsen, F. D., Van Eyk, J. E., Hodges, R. S., & Sykes, B. D. (1992) *Biochemistry 31*, 8790−8798.
Stone, D., & Smillie, L. B. (1978) *J. Biol. Chem. 253*, 1137−1148.
Talbot, J. A., & Hodges, R. S. (1982) *Acc. Chem Res. 15*, 224−230.
Thompson, K. S., Vinson, C. R., & Freire, E. (1993) *Biochemistry 32*, 5491−5496.
Vinson, C. R., Sigler, P. B., & McKnight, S. L. (1989) *Science 246*, 911−916.
Wright, P. E., Dyson, H. J., & Lerner, R. A. (1988) *Biochemistry 27*, 7167−7175.
Zhou, N. E., Zhu, B.-Y., Kay, C. M., & Hodges, R. S. (1992a) *Biopolymers 32*, 419−426.
Zhou, N. E., Kay, C. M., & Hodges, R. S. (1992b) *J. Biol. Chem. 267*, 2664−2670.
Zhou, N. E., Kay, C. M., & Hodges, R. S. (1992c) *Biochemistry 31*, 5739−5746.
Zhou, N. E., Zhu, B.-Y., Kay, C. M., & Hodges, R. S. (1993) in *Peptides, Biology & Chemistry, Proceedings of the 1992 Chinese Peptide Symposium* (Du, Y. C., Tam, J. P., & Zhang, Y.-S., Eds.) pp 217-220, ESCOM Science Publishers, Leiden, The Netherlands.
Zhou, N. E., Monera, O. D., Kay, C. M., & Hodges, R. S. (1994a) *Protein Pept. Lett.* (in press).
Zhou, N. E., Kay, C. M., & Hodges, R. S. (1994b) *Protein Eng.* (in press).
Zhu, B.-Y., Zhou, N. E., Semchuk, P. D., Kay, C. M., & Hodges, R. S. (1992) *Int. J. Pept. Protein Res. 40*, 171−179.
Zhu, B.-Y., Zhou, N. E., Kay, C. M., & Hodges, R. S. (1993) *Protein Sci. 2*, 383−394.